

# An Efficient Method to Study Shielding Effectiveness of Rectangular Enclosure with Wire Penetration

Pu-Yu Hu and Xiao-Ying Sun

College of Communication Engineering  
Jilin University, Changchun, 130022, P.R. China  
18643125804@163.com, sunxy@jlu.edu.cn

**Abstract** — This paper presents a reliable and efficient analytical model to calculate the shielding effectiveness (SE) of a rectangular enclosure with wire penetration under plane wave illumination over frequency range of 0 to 2.5GHz. The wire is equivalent to monopole antenna, and the four-element lumped-parameter equivalent circuit for monopole antenna is established to represent the coupling process between electric field and the wire. Based on dynamic Green function, the approximate solution of the electric field distribution in the enclosure excited by the internal wire is derived, and Bethe's theory is used to calculate the approximate solution of the electric field distribution in the enclosure excited by the aperture when the aperture size is not negligible. Several cases are presented to verify the validity of the model. The effects of the length of the wire inside and outside the enclosure, wire penetration and observation point position as well as incident direction of plane wave on the SE are discussed in detail. Simulation result of the proposed model are in good agreement with that of the transmission line matrix (TLM) method.

**Index Terms** — Equivalent dipole, rectangular enclosure, shielding effectiveness, wire penetration.

## I. INTRODUCTION

Shielding is one of the most important technologies in electromagnetic compatibility, which is widely used to protect electronic equipment from external electromagnetic radiation interference [1]. There is great interest in determination of shielding performance of the metallic enclosure, which is quantified by shielding effectiveness (SE). In real devices, there always exist aperture and wire penetration on the shielding enclosure to meet with internal electronic equipment power supply, data transmission and other practical needs. The external wire will induce external electromagnetic energy, and couple to the enclosure through internal wire. Meanwhile, when the size of the wire-penetrated aperture is big enough, aperture will also be an important electromagnetic coupling path and cannot be ignored. These two coupling paths will greatly reduce the shielding performance of

the shielding enclosure [2]. For these reasons, the study of the coupling effect of the enclosure with wire penetration becomes necessary in the shielding enclosure design.

The SE can be directly measured by the experiment [3, 4]. However, the experiment method is inefficient and expensive, which limits its applicability. Generally, numerical methods [5-7] and analytical formulations [8] are main ways to calculate SE. Numerical methods are suitable for calculating the SE of complex structures. Compared to numerical methods, analytical formulations require far less computational cost and are more suitable for regularity research. Zheng et al. applied Norton's equivalence theorem to study the electromagnetic coupling of an incident plane wave through a wire-penetrated electrically small aperture in an infinite conducting screen [9]. A transmission line model of the structure composed by a semi-infinite metallic screen with wire penetration on the ground plane was derived based on the scattering parameter by Daniele et al. [10]. Thomas et al. proposed a very efficient model to compute the coupling of external electromagnetic fields to the contents of an enclosure via wire penetrations using multiple-mode transmission line theory. The simulation results indicated a good consistency with the experimental data [11-13]. In this model, the wire was connected to enclosure through BNC connectors, and therefore the coupling effect of the wire-penetrated aperture was not taken into account. But in some applications, wires of the electronic device inside an enclosure will pass through the enclosure directly through aperture without connectors. Leone and Monich provided inductive coupling model and resonant dipole-antenna model to study the radiation of the enclosure by both wire and aperture [14]. Lertsirimit et al. developed an efficient hybrid method for analyzing the coupling to printed circuit board inside an enclosure via wire penetration using a combination of transmission-line analysis and full-wave solver [15]. Li solved the similar problem by a hybrid numerical analysis method of the partial element equivalent circuit (PEEC) and the method of moment (MoM), and the results of the hybrid

method were in good agreement with those of test [16].

In this paper, a reliable and efficient analytical model is developed to calculate the SE of rectangular enclosure with wire penetration under plane wave illumination. The coupling of external electromagnetic fields to an enclosure via both wire and wire-penetrated aperture is considered. The SE at any point within enclosure can be calculated efficiently and reliably. Simulation results of the presented model are in good agreement with that of the CST software over a wide frequency range (0~2.5GHz), which verifies the validity of the model. The effects of the length of the wire inside and outside the enclosure, wire penetration and observation point position as well as incident direction of plane wave on the SE are discussed in detail based on the model.

## II. ANALYTICAL MODEL

The physical structure of a metallic rectangular enclosure with a  $z$ -direction wire penetration is depicted in Fig. 1. The dimensions of the rectangular enclosure are  $x_e \times y_e \times z_e$ . The whole wire can be divided into two segments, named wire A and wire B. The length of the wire A outside the enclosure is  $l_A$  and the length of the wire B inside the enclosure is  $l_B$ . The radius of the wire and aperture are  $r_d$  and  $r_a$ . The penetration point of the wire is located at  $W(x_a, y_a, 0)$ , and the central position of the internal wire is located at  $S(x_a, y_a, l_B/2)$ . The monitor point is located at  $P(x_p, y_p, z_p)$  within the enclosure.

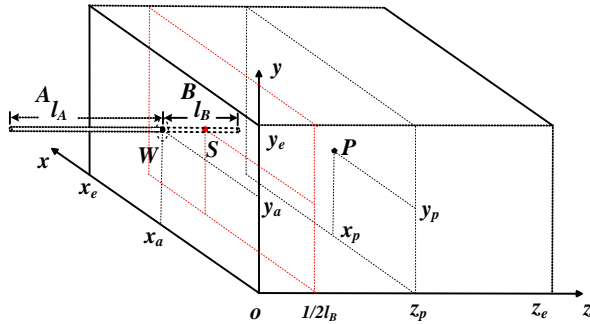


Fig. 1. Geometry of an enclosure with a wire penetration.

The enclosure is irradiated by an oblique plane wave with arbitrary incidence and polarization direction, as shown in Fig. 2. The electric field strength components of the plane wave can be described as:

$$E_x = E_0 \sin \alpha \sin \varphi + \cos \alpha \cos \varphi \sin \vartheta, \quad (1)$$

$$E_y = E_0 \cos \alpha \cos \vartheta, \quad (2)$$

$$E_z = E_0 \cos \alpha \sin \varphi \sin \vartheta - \sin \alpha \cos \varphi, \quad (3)$$

where  $E_0$  is the electric field amplitude,  $\varphi$  is azimuth angle,  $\vartheta$  is elevation angle and  $\alpha$  is polarization angle. The related H-field can be calculated by:

$$\mathbf{H} = \frac{1}{\eta} \mathbf{k} \times \mathbf{E}, \quad (4)$$

where  $\mathbf{k}$  is the wave vector direction vector, and  $\eta$  is the characteristic impedance of the medium.

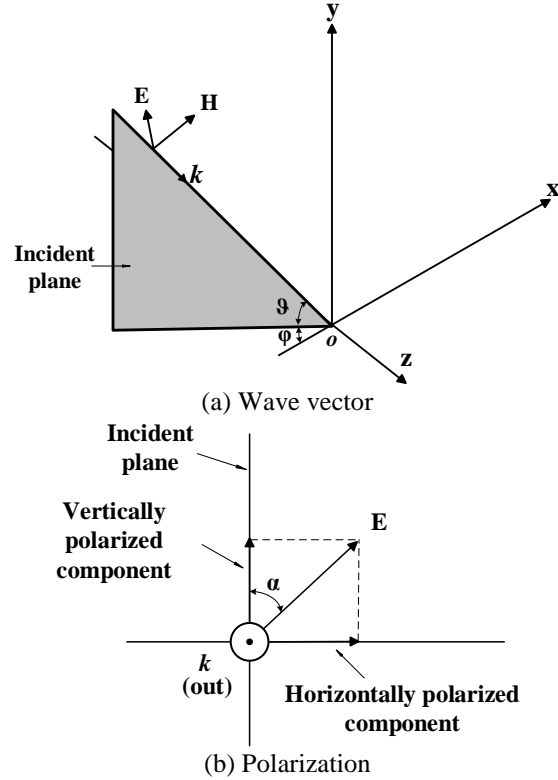


Fig. 2. Definition of the plane wave.

### A. Analytical model of wire

Assuming that the wire-penetrated aperture is small enough and can be ignored, the external wire is the main way to couple the electromagnetic energy. The coupling of electromagnetic energy to the enclosure is achieved by the internal wire. In order to calculate the induced energy of the external wire, we consider the wire as monopole antenna. For a dipole or monopole antenna, it can be modelled as an equivalent circuit containing frequency dependent lumped elements over a wide frequency range [17]. The geometry and the four-element circuit model of a dipole antenna are shown in Fig. 3. The length and the diameter of the dipole antenna are  $2h$  and  $2r$  respectively. The equivalent circuit consists of the capacitance  $C_0$  in series with a frequency dependent resistance called radiation resistance which is formed from a parallel connection circuit of  $C_1$ ,  $R_1$  and  $L_1$ . The equivalent impedance of the circuit is expressed as:

$$Z_d(j\omega) = \frac{1}{j\omega C_0} + \frac{j\omega(1/C_1)}{j\omega(1/C_1 R_1) + (1/L_1 C_1) - \omega^2}. \quad (5)$$

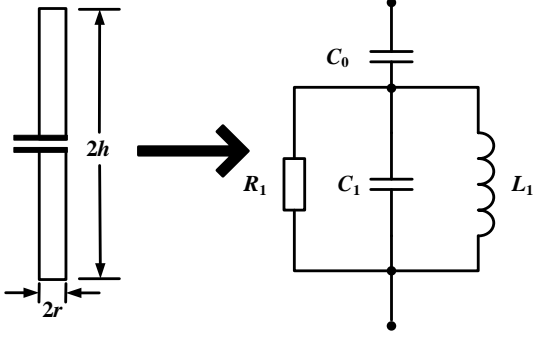


Fig. 3. The equivalent circuit model of a dipole antenna.

The values of  $R_1$ ,  $C_0$ ,  $C_1$ , and  $L_1$  up to the full-wave resonant frequency are given by [12]:

$$R_1 \approx [578.626] \ln(h/r) - [1675.1817] \Omega, \quad (6)$$

$$C_0 \approx [31.85] h / (\ln(h/r) - [0.6943]) \text{ pF}, \quad (7)$$

$$C_1 \approx [9.433] h / (\ln(h/r) - [2.458]) \text{ pF}, \quad (8)$$

$$L_1 \approx h ([119.58] \ln(h/r) - [147.07]) \text{ nH}, \quad (9)$$

where the contents in the square brackets represent empirical values.

The effective length of dipole antenna is given by [11]:

$$h_e(j\omega) = h\omega_h^2 / (\omega_h^2 + 2j\omega\delta_h - \omega^2), \quad (10)$$

where  $\omega_h = 2\pi f_h$ ,  $f_h$  is expressed as:

$$f_h \approx ([7.609] \ln(h/r) + [92.57]) / h \text{ MHz}, \quad (11)$$

the damping frequency  $\delta_h$  is expressed as:

$$\delta_h \approx \frac{h\omega_h}{2|he|_{\max}} \text{ rads/s}, \quad (12)$$

where  $|he|_{\max}$  is:

$$|he|_{\max} \approx h ([0.7063] \ln(h/r) + [0.1387]). \quad (13)$$

For a monopole above ground the self-impedance and effective length is exactly half of that given by (5) and (13) where  $h$  is the monopole length [11]. So the self-impedance  $Z_A$  and  $Z_B$  of the wire A and B are half of that obtained by substituting  $l_A$ ,  $l_B$  and  $r_d$  into formula (5)-(9), and the effective length  $h_{Ae}$  of the wire A is half of that obtained by substituting  $l_A$  and  $r_d$  into formula (10)-(13). Finally, the source current of the wire can be approximately expressed as [11]:

$$I_s = \frac{E_z h_{Ae}(j\omega)}{Z_A + Z_B}. \quad (14)$$

When the length of the internal wire is less than the wavelength, we neglect the influence of the current distribution of wire B and the complex coupling process between the aperture and the wire, the wire B is approximately equivalent to a  $z$ -direction electric dipole inside the enclosure with dipole effective length  $h_{Be}$  and current source  $I_s$  at the central position of the internal

wire. The electric field  $E$  in a rectangle enclosure contributed by the electric current distributions  $J$  inside the enclosure can be represented as [18]:

$$E(r) = -j\omega\mu_0 \iiint_V G_e(r, r') J(r') dV', \quad (15)$$

where  $\mu_0$  is the permeability of the medium,  $G_e$  is the dyadic Green's function, and  $V$  is the volume which sources occupy.

The electric field components at point  $P(x_p, y_p, z_p)$ , which are excited by the  $z$ -direction equivalent electric dipole located at the central position of the internal wire  $S(x_a, y_a, l_B/2)$ , are given by [19]:

$$E_{sz}(x_p, y_p, z_p) = \frac{-\varepsilon_{0m}\varepsilon_{0n}j\omega\mu_0(h_{Be}I_s)}{2k^2(x_e y_e)} \cdot \sum_{m=0}^{\infty} \sum_{n=0}^{\infty} \left\{ \frac{\Gamma_{mn} \cos k_{mn}(z_p + l_B/2 - z_e)}{k_{mn} \sin(k_{mn} z_e)} + \frac{\Gamma_{mn} \cos k_{mn}(|z_p - l_B/2| - z_e)}{k_{mn} \sin(k_{mn} z_e)} \right\}, \quad (16)$$

$$E_{sy}(x_p, y_p, z_p) = \frac{-\varepsilon_{0m}\varepsilon_{0n}j\omega\mu_0(h_{Be}I_s)}{2k^2(x_e y_e)} \cdot \sum_{m=0}^{\infty} \sum_{n=0}^{\infty} \left\{ \frac{\Gamma'_{mn} \sin k_{mn}(z_e - z_p - l_B/2)}{\sin(k_{mn} z_e)} + \frac{\Gamma'_{mn} \operatorname{sgn}(z_p - l_B/2) \sin k_{mn}(z_e - |z_p - l_B/2|)}{\sin(k_{mn} z_e)} \right\}, \quad (17)$$

$$E_{sx}(x_p, y_p, z_p) = \frac{-\varepsilon_{0m}\varepsilon_{0n}j\omega\mu_0(h_{Be}I_s)}{2k^2(x_e y_e)} \cdot \sum_{m=0}^{\infty} \sum_{n=0}^{\infty} \left\{ \frac{\Gamma''_{mn} \sin k_{mn}(z_e - z_p - l_B/2)}{\sin(k_{mn} z_e)} + \frac{\Gamma''_{mn} \operatorname{sgn}(z_p - l_B/2) \sin k_{mn}(z_e - |z_p - l_B/2|)}{\sin(k_{mn} z_e)} \right\}, \quad (18)$$

where

$$k_{mn} = \sqrt{k^2 - (m\pi/x_e)^2 - (n\pi/y_e)^2}, \quad (19)$$

$$\Gamma_{mn} = \left[ (m\pi/x_e)^2 + (n\pi/y_e)^2 \right] \sin(m\pi x_a/x_e) \cdot \sin(n\pi y_a/y_e) \sin(m\pi x_p/x_e) \sin(n\pi y_p/y_e), \quad (20)$$

$$\Gamma'_{mn} = (n\pi/y_e) \sin(m\pi x_a/x_e) \sin(n\pi y_a/y_e) \cdot \sin(m\pi x_p/x_e) \cos(n\pi y_p/y_e), \quad (21)$$

$$\Gamma''_{mn} = (m\pi/x_e) \sin(m\pi x_a/x_e) \sin(n\pi y_a/y_e) \cdot \cos(m\pi x_p/x_e) \sin(n\pi y_p/y_e), \quad (22)$$

where  $\operatorname{sgn}(\ )$  represents sign function.  $\varepsilon_{0m}$  and  $\varepsilon_{0n}$  are Neumann factors which can be expressed as:

$$\varepsilon_{0m} = \begin{cases} 1, & m = 0 \\ 2, & m \neq 0 \end{cases}, \quad (23)$$

$$\varepsilon_{0n} = \begin{cases} 1, & n = 0 \\ 2, & n \neq 0 \end{cases}. \quad (24)$$

The electric field and SE at observation point are:

$$E_{ps} = \sqrt{(E_{sx})^2 + (E_{sy})^2 + (E_{sz})^2}, \quad (25)$$

$$SE_{ps} = -20 \log_{10} |E_{ps} / E_0|. \quad (26)$$

### B. Analytical model of wire-penetrated aperture

When the size of the wire-penetrated aperture is big enough, the leakage electric field from wire-penetrated aperture cannot be ignored and need to be considered. Here we ignore the complex coupling relations between the wire and aperture, and the total electric field at point  $P(x_p, y_p, z_p)$  inside the enclosure is expressed as:

$$E_t = E_{ps} + E_{pa}, \quad (27)$$

where  $E_{pa}$  is the leakage electric field from wire-penetrated aperture without wire, as shown in Fig. 4.

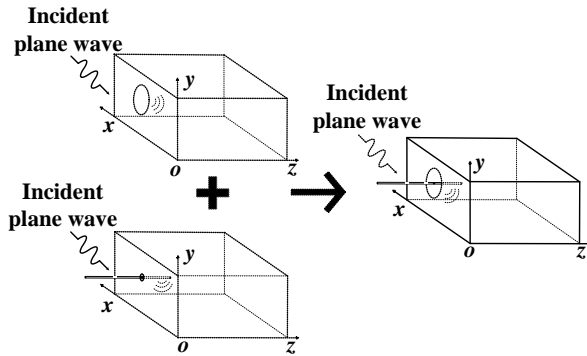


Fig. 4. The coupling of electric fields to the enclosure via both wire and wire-penetrated aperture.

We apply Bethe's theory and replace the aperture with electric and magnetic dipoles located on both sides of the perfectly electric conducting surface which fill the aperture [20]. The electric dipole  $\mathbf{p}$  and magnetic dipoles  $\mathbf{m}$  are outside the completely closed enclosure, while the mirrored dipoles  $\mathbf{m}'$  and  $\mathbf{p}'$  are inside the enclosure, as shown in Fig. 5.

The electric dipole is normal to the plane of the aperture, and the magnetic dipoles are parallel to the plane of the aperture. Dipole strengths are given by [19]:

$$\mathbf{p} = \mathbf{p}' = \alpha_e \varepsilon_0 E_{SCz} \hat{\mathbf{z}}, \quad (28)$$

$$\mathbf{m} = \mathbf{m}' = -\alpha_{mx} H_{SCx} \hat{\mathbf{x}} - \alpha_{my} H_{SCy} \hat{\mathbf{y}}, \quad (29)$$

where  $\varepsilon_0$  is the dielectric constant.  $E_{SC}$  and  $H_{SC}$  are the short circuited electric field and magnetic field at the perfectly electric conducting surface in the absence of the aperture, which are two times of the electric field and magnetic field of the incident plane wave. For a circular

aperture with radius of  $r_a$ , the magnetic polarizabilities  $\alpha_{mx}$ ,  $\alpha_{my}$  and electric polarizabilities  $\alpha_e$  are given by:

$$\alpha_e = 2r_a^3 / 3, \quad (30)$$

$$\alpha_{mx} = \alpha_{my} = 4r_a^3 / 3. \quad (31)$$

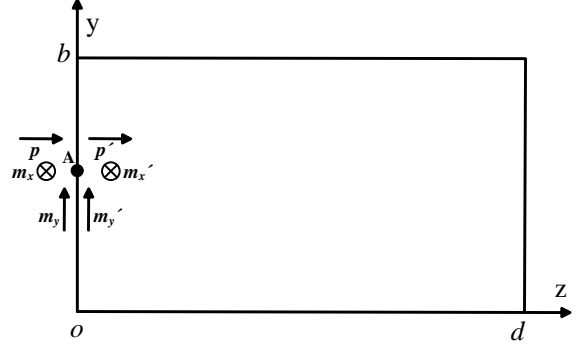


Fig. 5. Enclosure with equivalent dipole located at both sides of the wire-penetrated aperture.

The electric field components at point  $P(x_p, y_p, z_p)$ , which are excited by the  $z$ -direction electric dipole inside a completely closed enclosure located at the center point of the wire-penetrated aperture  $W(x_a, y_a, 0)$ , are [19]:

$$E_{ez}(x_p, y_p, z_p) = \frac{-\varepsilon_{0m} \varepsilon_{0n} j \omega \mu_0 (j \omega p')}{k^2(x_e y_e)} \cdot \sum_{m=0}^{\infty} \sum_{n=0}^{\infty} \frac{\Gamma_{mn}}{k_{mn}} \frac{\cos(k_{mn}(z_p - z_e))}{\sin(k_{mn} z_e)}, \quad (32)$$

$$E_{ey}(x_p, y_p, z_p) = \frac{-\varepsilon_{0m} \varepsilon_{0n} j \omega \mu_0 (j \omega p')}{k^2(x_e y_e)} \cdot \sum_{m=0}^{\infty} \sum_{n=0}^{\infty} \Gamma'_{mn} \frac{\sin(k_{mn}(z_e - z_p))}{\sin(k_{mn} z_e)}, \quad (33)$$

$$E_{ex}(x_p, y_p, z_p) = \frac{-\varepsilon_{0m} \varepsilon_{0n} j \omega \mu_0 (j \omega p')}{k^2(x_e y_e)} \cdot \sum_{m=0}^{\infty} \sum_{n=0}^{\infty} \Gamma''_{mn} \frac{\sin(k_{mn}(z_e - z_p))}{\sin(k_{mn} z_e)}. \quad (34)$$

The electric field components excited by the  $x$ -direction magnetic dipole are given by [21, 22]:

$$E_{mxz}(x_p, y_p, z_p) = \frac{\varepsilon_{0m} \varepsilon_{0n} j \omega \mu_0 m'_x}{x_e y_e} \cdot \sum_{m=0}^{\infty} \sum_{n=0}^{\infty} \frac{\Gamma'_{MNx}}{k_{mn}} \frac{\cos(k_{mn}(z_p - z_e))}{\sin(k_{mn} z_e)}, \quad (35)$$

$$E_{mxy}(x_p, y_p, z_p) = \frac{\varepsilon_{0m} \varepsilon_{0n} j \omega \mu_0 m'_x}{x_e y_e} \cdot \sum_{m=0}^{\infty} \sum_{n=0}^{\infty} \Gamma''_{MNx} \frac{\sin(k_{mn}(z_e - z_p))}{\sin(k_{mn} z_e)}, \quad (36)$$

$$E_{mxx}(x_p, y_p, z_p) = 0, \quad (37)$$

where

$$\Gamma'_{MNx} = \frac{n\pi}{y_e} \sin\left(\frac{m\pi x_a}{x_e}\right) \cos\left(\frac{n\pi y_a}{y_e}\right) \cdot \sin\left(\frac{m\pi x_p}{x_e}\right) \sin\left(\frac{n\pi y_p}{y_e}\right), \quad (38)$$

$$\Gamma''_{MNx} = \sin\left(\frac{m\pi x_a}{x_e}\right) \cos\left(\frac{n\pi y_a}{y_e}\right) \cdot \sin\left(\frac{m\pi x_p}{x_e}\right) \cos\left(\frac{n\pi y_p}{y_e}\right). \quad (39)$$

Similarly, we can easily calculate the value of  $E_{myz}$ ,  $E_{myy}$  and  $E_{myx}$  due to the  $y$ -direction magnetic dipole.

The total leakage electric field components from the aperture and wire at observation point  $P(x_p, y_p, z_p)$  can be obtained by:

$$E_{tx} = E_{sx} + E_{ex} + E_{mxx} + E_{myx}, \quad (40)$$

$$E_{ty} = E_{sy} + E_{ey} + E_{mxy} + E_{myy}, \quad (41)$$

$$E_{tz} = E_{sz} + E_{ez} + E_{mxz} + E_{myz}. \quad (42)$$

The total electric field and SE at  $P(x_p, y_p, z_p)$  are:

$$E_t = \sqrt{(E_{tx})^2 + (E_{ty})^2 + (E_{tz})^2}, \quad (43)$$

$$SE_t = -20 \log_{10} |E_t / E_0|. \quad (44)$$

### III. EXAMPLE AND ANALYSIS

In this section, the simulation results of the proposed model are compared with the results of the CST software based on transmission line matrix (TLM) method covering frequency range 0~2.5GHz. In TLM simulation, the material of the rectangle enclosure is aluminum with conductivity of  $3.56 \times 10^7$  S/m, and the dimension of the enclosure are  $x_e \times y_e \times z_e = 300\text{mm} \times 260\text{mm} \times 120\text{mm}$ . The wire is good conductor with a radius of 4mm. Boundary conditions are set to absorbing boundary. We set the plane wave as the excitation source and electric field probes to calculate the electric field within the enclosure. Automatic meshing is adopted, and the accuracy is set to -80dB. Six cases are considered to verify the validity of the model, with various external and internal wire length, penetration point position, observation point position, incident direction of the plane wave and aperture radius listed in Table 1.

Table 1: Specific parameter settings

Case	External and Internal Wire Length (mm) ( $l_A, l_B$ )	Aperture Radius (mm) $r_a$	Wire Penetration Point Position (mm) ( $x_a, y_a$ )	Observation Point Positions (mm) ( $x_p, y_p, z_p$ )	Elevation Angle ( $^\circ$ ) $\vartheta$
1	(80, 50)	4.1	(150, 100)	(150, 215, 60)	90
2	(80, 50)	4.1	(225, 140)	(65, 90, 70)	90
3	(60/100, 50)	4.1	(150, 100)	(150, 215, 60)	90
4	(80, 10/30)	4.1	(150, 100)	(150, 215, 60)	90
5	(80, 50)	4.1	(150, 100)	(150, 215, 60)	20/45
6	(80, 50)	30	(150, 100)	(150, 215, 60)	90

Cases 1-5 are designed to study the coupling of electromagnetic field to the enclosure achieved by wire. We set the radius of the wire-penetrated aperture to 4.1mm, which is small enough to ignore the leakage electric field from aperture. Case 6 is designed to study the coupling of electromagnetic field to the enclosure obtained by both wire and aperture.

For case 1, the length of the external wire  $A$  and internal wire  $B$  are 80mm and 50mm respectively. The plane wave travels uniformly along the negative direction of the  $y$ -axis, with azimuth angle  $\varphi=90^\circ$ , elevation angle  $\vartheta=90^\circ$ , and polarization angle  $\alpha=0^\circ$ . The electric field is parallel to the external wire which is the worst case for shielding according to the formula (14). The simulation results of the proposed model and TLM method are shown in Fig. 6. The results obtained from the two methods are nearly the same, except discrepancies at low frequency. This may be due to the neglect of the current distribution of the internal wire and the complex

coupling process between the aperture and the wire in the model. SE results of the enclosure with aperture radius of 4.1mm and without wire are also shown in Fig. 6. Comparing the results under two conditions, we can see that the coupled electric field from the wire will lead to a significant reduction in SE of the enclosure, for example the reduction is 40dB at 500MHz. The leakage electric field from aperture is very few, which prove that we can just ignore it.

For case 2, penetration point and observation point position have changed compared to case 1. The simulation results of the proposed model and TLM method are shown in Fig. 7. The comparison between two methods demonstrates that the proposed method is applicable and effective. Compared with the results of case 1 and case 2, it can be found that the change of penetration point and observation point position has a little influence on the amplitude of the SE, but some higher order resonant modes will occur.

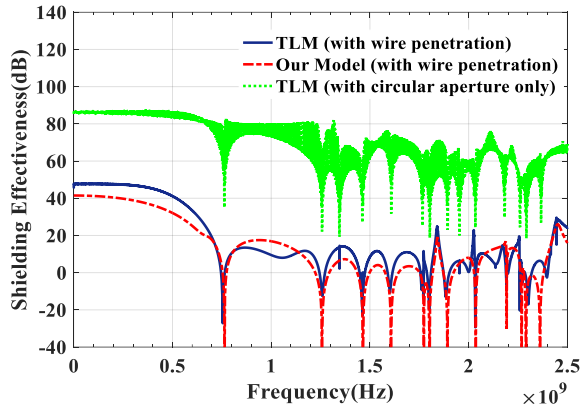


Fig. 6. SE result of case 1.

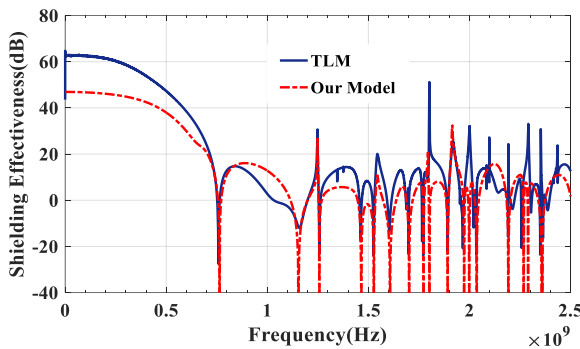


Fig. 7. SE result of case 2.

For case 3, the trend of SE along with change of the length of the external wire is analyzed. Here we select the model of case 1, and the lengths of the external wire are 60mm and 100mm respectively. From the simulation results shown in Fig. 8 and Fig. 9, we can see that the proposed model and TLM method are in good agreement. Combined with the results of case 1, we can find that as the external wire length decreases, the SE of the enclosure increases continuously within 1GHz. But at frequencies higher than about 1.25GHz, the SE of the enclosure gradually decreases with the decrease of external wire length, as shown in Fig. 10.

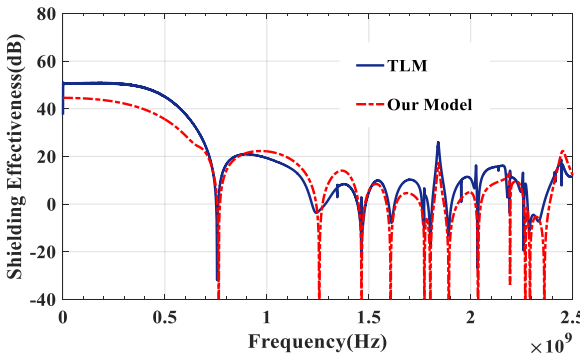


Fig. 8. SE result of case 3 ( $l_A=60\text{mm}$ ).

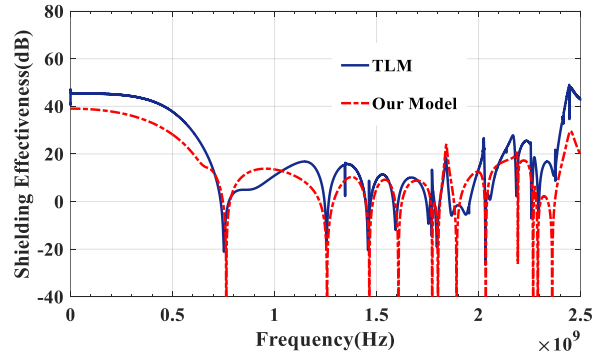


Fig. 9. SE result of case 3 ( $l_A=100\text{mm}$ ).

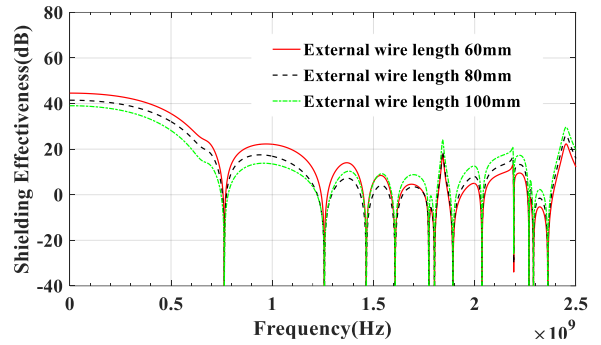


Fig. 10. SE results of the enclosure with different external wire length.

For case 4, the trend of SE along with change of the length of the internal wire is discussed. The enclosure model in case 1 is selected, the lengths of the internal wire are 10mm and 30mm respectively. The simulation results of the proposed model and TLM method are shown in Fig. 11 and Fig. 12. Simulation results show a good consistency between the two methods. Combined with the results of case 1, we can conclude that as the internal wire length decreases, the SE of the enclosure will increase continuously, as shown in Fig. 13. In comparison with case 3, we can find that the influence of the internal wire on SE is larger than that of external wire.

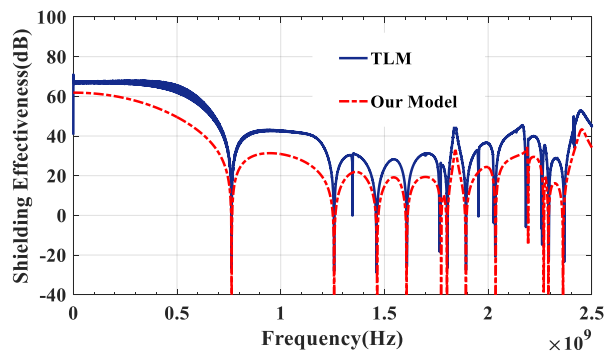


Fig. 11. SE result of case 4 ( $2l_B=10\text{mm}$ ).

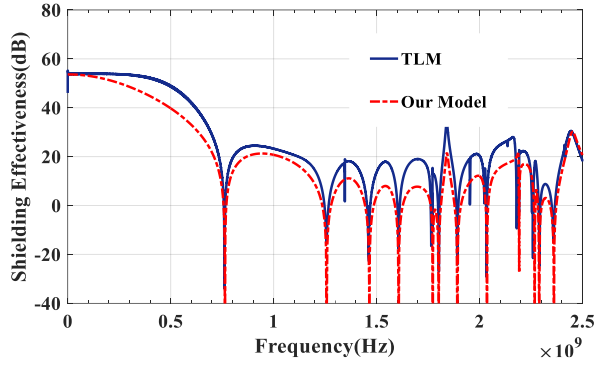


Fig. 12. SE result of case 4 ( $2l_B=30\text{mm}$ ).

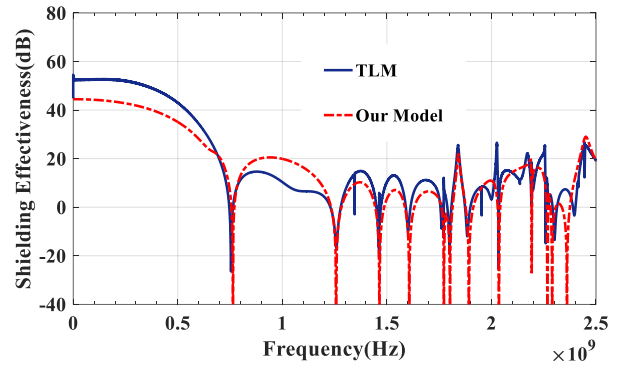


Fig. 15. SE result of case 5 (Elevation angle is  $45^\circ$ ).

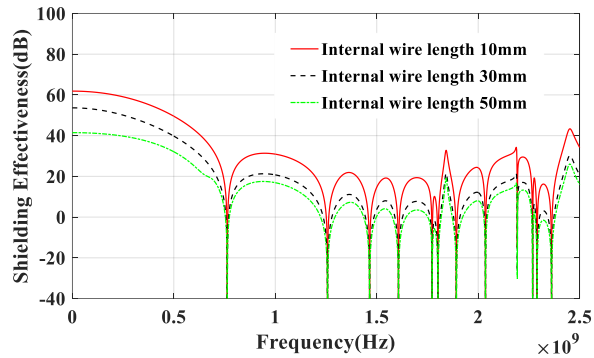


Fig. 13. SE results of the enclosure with different internal wire length.

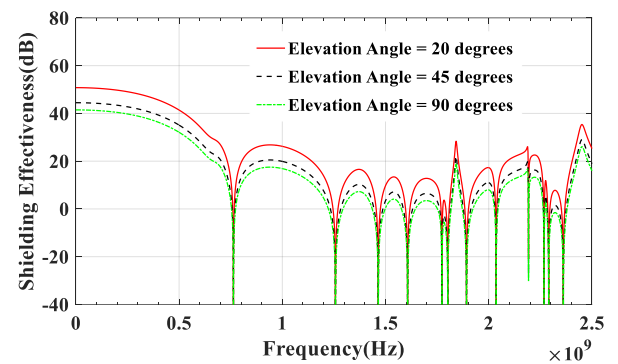


Fig. 16. SE results of the enclosure with different elevation angle.

For case 5, the influence of elevation angle on SE under vertical polarization is discussed. The model of case 1 is selected, here we set the elevation angles to 20 and 45 degrees. The simulation results shown in Fig. 14 and Fig. 15 show that the SE derived from the proposed model are basically consistent with that of TLM method, and as the elevation angle decreases, the SE of the enclosure will increase continuously. The worst case for shielding is when electric field parallel to the external wire, as shown in Fig. 16.

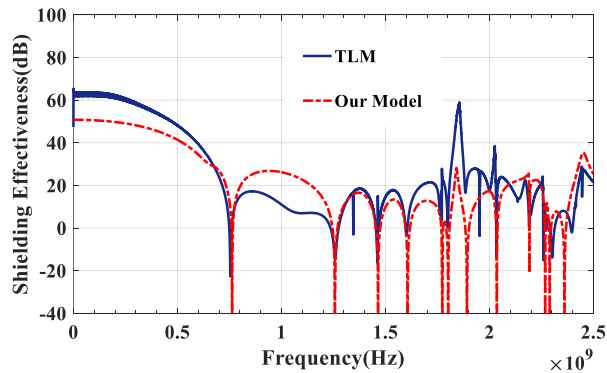


Fig. 14. SE result of case 5 (Elevation angle is  $20^\circ$ ).

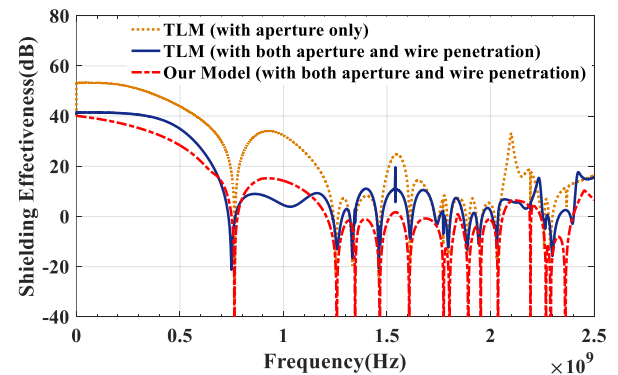


Fig. 17. Comparison of the SE results of the enclosure with both wire and aperture and with aperture only.

For case 6, the effect of aperture is taken into account. When the size of the aperture is big enough, the coupling of external electromagnetic fields to the enclosure via both wire and aperture need to be considered. Here we select the model of case 1. The radius of the circular aperture is  $r_a=30\text{mm}$ . From the simulation results of the proposed model and TLM method shown in Fig. 17, we can see that the two methods also have a good agreement and wire-

penetration significantly reduces the SE of the enclosure, especially at low frequency. In such a case, the SE of the enclosure with wire and aperture is reduced by about 10dB-20dB compared with the SE of the enclosure with aperture only at frequencies below 1.25GHz.

#### IV. CONCLUSION

In order to study the shielding performance of a metallic rectangular enclosure with wire penetration, we present a novel analytical model in this paper. The couplings of external electromagnetic fields to the enclosure via both wire and aperture are analyzed using monopole antenna equivalent circuit modeling and Bethe's theory. Various parameters such as the length of the wire inside and outside the enclosure, wire penetration and observation point position as well as incident direction of plane wave are taken into account. By this model, the SE of the enclosure with wire penetration under plane wave illumination can be calculated quickly and accurately over a wide frequency range (0~2.5G). Several cases have been presented to demonstrate the validity and accuracy of the model. The overall simulation results of the model match well with those of CST simulation software using TLM method, expect discrepancies existing at low frequency. The analysis shows that (1) the wire penetration will greatly reduce the SE of the enclosure; (2) both the length of the wire inside and outside the enclosure will affect the SE of the enclosure, but the influence of the internal wire on SE is larger than that of external wire. The SE decreases with the increase of the length of internal wire; (3) the condition where electric field is parallel to the external wire is the worst case for shielding. Compared with TLM method and other numerical algorithms, the proposed method has higher computation speed and higher computational efficiency, and therefore has its values on shielding enclosure design.

#### REFERENCES

- [1] T. Cvetkovic, V. Milutinovic, N. Doncov, and B. Milovanovic, "Numerical investigation of monitoring antenna influence on shielding effectiveness characterization," *Appl. Comp. Electro. Society (ACES) Journal*, vol. 29, no. 11, pp. 837-846, Nov. 2014.
- [2] G. Manara, M. Bandinelli, and A. Monorchio, "Electromagnetic penetration and coupling to wires through apertures of arbitrary shape," *IEEE Trans. Electromagn. Compat.*, vol. 40, no. 4, pp. 391-396, Nov. 1998.
- [3] S. Z. Sapuan and M. Z. M. Jenu, "Shielding effectiveness and S21 of a rectangular enclosure with aperture and wire penetration," *2007 Asia-Pacific Conference on Applied Electromagnetics*, pp. 1-5, Dec. 2007.
- [4] K. Yusoff, M. Z. M. Jenu, W. R. W. Abdullah, and B. M. Shariff, "Experimental study of the electromagnetic coupling to an enclosure via a wire penetration," *2005 Asia-Pacific Conference on Applied Electromagnetics*, pp. 172-174, Dec. 2005.
- [5] S. T. Song, H. Jiang, and Y. L. Huang, "Simulation and analysis of HEMP coupling effect on a wire inside an apertured cylindrical shielding cavity," *Appl. Comp. Electro. Society (ACES) Journal*, vol. 27, no. 6, pp. 505-515, June 2012.
- [6] R. Araneo and G. Lovat, "Analysis of the shielding effectiveness of metallic enclosures excited by internal sources through an efficient method of moment approach," *Appl. Comp. Electro. Society (ACES) Journal*, vol. 25, no. 7, pp. 600-611, July 2010.
- [7] G. Wu, Z. Q. Song, X. G. Zhang, and B. Liu, "Study on coupling characteristics of electromagnetic wave penetrating metallic enclosure with rectangular aperture," *Appl. Comp. Electro. Society (ACES) Journal*, vol. 26, no. 7, pp. 611-618, July 2011.
- [8] C. C. Wang, C. Q. Zhu, X. Zhou, and Z. F. Gu, "Calculation and analysis of shielding effectiveness of the rectangular enclosure with apertures," *Appl. Comp. Electro. Society (ACES) Journal*, vol. 28, no. 6, pp. 535-545, June 2013.
- [9] E. Zheng, R. F. Harrington, and J. R. Mautz, "Electromagnetic coupling through a wire-penetrated small aperture in and infinite conducting plane," *IEEE Trans. Electromagn. Compat.*, vol. 35, no. 2, pp. 295-300, May 1993.
- [10] V. Daniele, M. Gilli, and S. Pignari, "EMC prediction model of a single wire transmission line crossing a circular aperture in a planar screen," *IEEE Trans. Electromagn. Compat.*, vol. 38, no. 2, pp. 117-126, May 1996.
- [11] D. W. P. Thomas, A. Denton, T. M. Benson, and C. Christopoulos, "Electromagnetic coupling to an enclosure via a wire penetration," *IEEE Int. Symp. on Electromagn. Compat.*, pp. 183-188, Aug. 2001.
- [12] A. Nanni, D. W. P. Thomas, C. Christopoulos, T. Konefal, J. Paul, and L. Sandrolini, et al., "Electromagnetic coupling between wires and loops inside a rectangular cavity using multiple-mode transmission line theory," *IEEE Int. Symp. on Electromagn. Compat.*, pp. 609-614, Sep. 2004.
- [13] T. Konefal, J. F. Dawson, A. C. Denton, and T. M. Benson, et al., "Electromagnetic coupling between wires inside a rectangular cavity using multiple-mode-analogous-transmission-line circuit theory," *IEEE Trans. Electromagn. Compat.*, vol. 43, no. 3, pp. 273-281, Aug. 2001.
- [14] M. Leone and G. Monich, "Coupling of apertures in enclosures to external cabling structures," *IEEE*

- Trans. Electromagn. Compat.*, vol. 46, no. 1, pp. 107-110, Feb. 2004.
- [15] C. Lertsirimit, D. R. Jackson, and D. R. Wilton, "An efficient hybrid method for calculating the EMC coupling to a device on a printed circuit board inside a cavity by a wire penetrating an aperture," *Electromagnetics*, vol. 25, no. 7-8, pp. 637-654, Oct. 2005.
- [16] P. Li, F. R. Yang, and W. Y. Xu, "An efficient approach for analyzing shielding effectiveness of enclosure with connected accessory based on equivalent dipole modeling," *IEEE Trans. Electromagn. Compat.*, vol. 58, no. 1, pp. 103-110, Feb. 2016.
- [17] T. G. Tang, Q. M. Tieng, and M. W. Gunn, "Equivalent circuit of a dipole antenna using frequency-independent lumped elements," *IEEE Trans. Antennas Propag.*, vol. 41, no. 1, pp. 100-103, Jan. 1993.
- [18] L. W. Li, P. S. Kooi, M. S. Leong, and T. S. Yeo, "On the eigenfunction expansion of electromagnetic dyadic green's functions in rectangular cavities and waveguides," *IEEE Trans. Microw. Theory Tech.*, vol. 43, no. 3, pp. 700-702, Mar. 1995.
- [19] F. M. Tesche, M. V. Ianoz, and T. Karlsson, *EMC Analysis Methods and Computational Models*. Wiley, New York, 1997.
- [20] P. Y. Hu and X. Y. Sun, "Study of the calculation method of shielding effectiveness of rectangle enclosure with an electrically large aperture," *Progress In Electromagnetics Research M*, vol. 61, pp. 85-96, 2017.
- [21] S. K. Goudos, E. E. Vafiadis, and J. N. Sahalos, "Monte Carlo simulation for the prediction of

the emission level from multiple sources inside shielded enclosures," *IEEE Trans. Electromagn. Compat.*, vol. 44, no. 2, pp. 291-308, May 2002.

- [22] R. J. H. Crawhall, "EMI potential of multiple sources within a shielded enclosure," University of Ottawa, Ph.D., 1993.



EMC and EM protection.

**Pu-Yu Hu** received the B.S. degree in Electronic and Information Engineering from Changchun University of Technology, China, in 2015. He is currently working toward the Ph.D. degree in Communication and Information System in Jilin University. His research interests include



**Xiao-Ying Sun** received the Ph.D. degrees in Communication and Information System from Jilin University, Jilin, China, in 2005. Now he is a Professor and the Dean of College of Communication Engineering in Jilin University, Changchun, Jilin, China.

From 1996 to 2004, he was a Lecturer in the School of Radio Engineering, Jilin University, China. From 2005 to 2009, he was an Associate Professor in the School of Communication Engineering, Jilin University, China. His research interests include EMC, EM protection, array signal processing and tactile representation.